Light Fragment Production and Power Law Behavior in Au + Au Collisions

S. Wang,[2] S. Albergo,[6] F. Bieser,[1] F. P. Brady,[4] Z. Caccia,[6] D. A. Cebra,[4] A. D. Chacon,[5] J. L. Chance,[4] Y. Choi,[3,*] S. Costa,[6] J. B. Elliott,[3] M. L. Gilkes,[3,†] J. A. Hauger,[3] A. S. Hirsch,[3] E. L. Hjort,[3] A. Insolia,[6] M. Justice,[2] D. Keane,[2] J. Kintner,[4] M. A. Lisa,[1] H. S. Matis,[1] M. McMahan,[1] C. McParland,[1] D. L. Olson,[1] M. D. Partlan,[4] N. T. Porile,[3] R. Potenza,[6] G. Rai,[1] J. Rasmussen,[1] H. G. Ritter,[1] J. Romanski,[6] J. L. Romero,[4] G. V. Russo,[6] R. P. Scharenberg,[3] A. Scott,[2] Y. Shao,[2,‡] B. K. Srivastava,[3] T. J. M. Symons,[1] M. L. Tincknell,[3] C. Tuvè,[6] P. G. Warren,[3] D. Weerasundara,[2] H. H. Wieman,[1] and K. L. Wolf[5]

(EOS Collaboration)

[1]*Lawrence Berkeley Laboratory, Berkeley, California 94720*

[2]*Kent State University, Kent, Ohio 44242*

[3]*Purdue University, West Lafayette, Indiana 47907*

[4]*University of California, Davis, California 95616*

[5]*Texas A&M University, College Station, Texas 77843*

[6]*Università di Catania and INFN-Sezione di Catania, 95129 Catania, Italy*

(Received 29 August 1994)

Using charged-particle-exclusive measurements of Au + Au collisions in the LBL Bevalac's EOS time projection chamber, we investigate momentum-space densities of fragments up to ^{4}He as a function of fragment transverse momentum, azimuth relative to the reaction plane, rapidity, multiplicity, and beam energy. Most features of these densities above a transverse momentum threshold are consistent with momentum-space coalescence, and, in particular, the increase in sideward flow with fragment mass is generally well described by a momentum-space power law.

PACS numbers: 25.75.+r, 25.70.Pq

Measurements of single-particle-inclusive spectra from heavy-ion collisions indicate a simple empirical pattern of light fragment production: The observed invariant momentum-space density ρ_A for fragments with mass number A and momentum $A\mathbf{p}$ closely follows the Ath power of the observed proton density ρ_1^A at momentum $\mathbf{p}$. This power law behavior was found to hold for spectra of participant fragments up to $A = 14$ with projectiles ranging from protons to Au at a variety of beam energies between $0.1A$ and $15A$ GeV [1]. These observations are consistent with the following picture: Composite fragment formation is determined during the stage of *chemical freeze-out*, when the system has expanded and the rate of hard nucleon-nucleon scattering has decreased; at this stage, nucleons that by chance lie close to each other in position and velocity can coalesce into composite fragments [2]. In the present work, we test the momentum-space power law up to ^{4}He in Au + Au collisions, for the first time studying ρ_A as a function of fragment azimuth relative to the event reaction plane.

Many possible theories of the collision process are compatible with this power law, ranging from simple thermal models to elaborate microscopic approaches where the time evolution of the system is followed at the nucleon level [3]. However, the quantum molecular dynamics (QMD) model, which treats the full multinucleon phase space, indicates that dynamical correlations originating early in the time evolution can result in deviations from statistical coalescence and these deviations are negligible only in very violent collisions, e.g., central Au + Au events at several hundred A MeV and above [3,4]. Thus, we can expect to gain insight into the collision dynamics from a determination of the conditions where coalescence behavior holds as well as where it breaks down.

Because participant fragments generally obey the power law in momentum space alone, we can conclude that spatial density effects are independent of momentum. The simplest momentum-space coalescence model [2], which neglects differences between proton and neutron spectra and ignores spatial density effects, predicts that coalescence coefficients $C_A = \rho_A/\rho_1^A$ depend only on fragment type. An explicit treatment of spatial density through six-dimensional coalescence [5] can be useful if the number of participants varies. Assuming that the average spatial density at freeze-out varies little with the size of the system, we expect C to decrease if the number of participants increases, as occurs with an increase in the mass of the colliding ions or with an increase in the centrality of the collisions. This trend is indeed observed among the inclusive data [1], and the multiplicity dependence of abundance ratios measured by the Plastic Ball is also consistent with six-dimensional coalescence [6].

This Letter is based on Au + Au data from the EOS time projection chamber (TPC) at Lawrence Berkeley Laboratory. This TPC is the principal subsystem of the EOS detector; it has rectangular geometry and operates in a 1.3 T magnetic field. Details about the detector and its performance can be found elsewhere [7–9]. We report results for fragments emitted forward of midrapidity,

 0031-9007/95/74(14)/2646(4)$06.00

where acceptance is optimum; our samples after multiplicity selection contain about 41 000 events at a beam energy of 1.15A GeV, and typically 6000 events each at 1.0A, 0.8A, 0.6A, and 0.25A GeV. Following the convention introduced by the Plastic Ball group, we characterize the centrality of collisions in terms of baryonic fragment multiplicity M as a fraction of $M_{\max}$, where $M_{\max}$ is a value near the upper limit of the M spectrum where the height of the distribution has fallen to half its plateau value [10]. Mult 1 through Mult 4 denote the four intervals of M with upper boundaries at 0.25, 0.5, 0.75, and 1.0 times $M_{\max}$, respectively, and Mult 5 denotes $M > M_{\max}$.

To assess the extent to which the momentum-space power law describes light composite fragment production in the EOS TPC, we first use our largest sample (1.15A GeV Au + Au) to test the agreement between the shapes of $\rho_A(x)$ and $\rho_1^A(x)$, where x is any observable such that ρ varies significantly over its range. The solid circles in the upper panels of Fig. 1 show the dependence on $p^\perp/A$ of the deuteron density $\rho_2 = A^2 dN_2/p^\perp dp^\perp$ for Mult 4 events in five intervals of center-of-mass rapidity y', where the prime denotes rapidity divided by the projectile rapidity ($y = 0.72y'$). The units of N_2 are deuterons per event per y' unit. We show the proton density as solid curves, and the proton density squared is given by the dashed curves, normalized

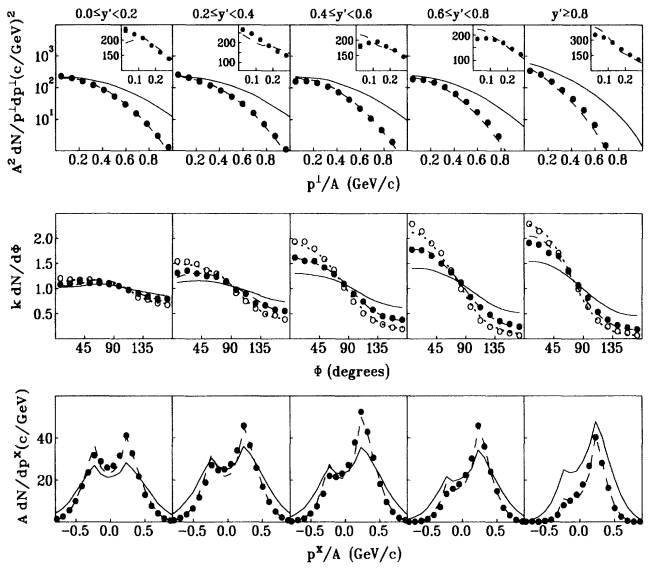

FIG. 1. Momentum-space density for deuterons (solid circles), protons (solid curves), and relative proton density squared (dashed curves) in Mult 4 collisions of 1.15A GeV Au + Au as a function of transverse momentum per nucleon (top), azimuth relative to the event reaction plane (center), and transverse momentum per nucleon projected on the reaction plane (bottom). In the center panels, the open circles indicate the density for fragments with $A = 3$ and the dotted curves the density for deuterons to the power of 3/2. In the bottom panels, the deuteron densities and proton densities squared were doubled before plotting.

to the same area as the deuteron density for this y' interval. This normalization is equivalent to optimizing coalescence coefficients C separately at each y'; the variation of C with y' is considered later. Statistical uncertainties approach the symbol size near the upper end of the $p^\perp/A$ scale, but are far smaller at the lower end. Accordingly, the insets in the upper right corners show the same data with better resolution at lower $p^\perp/A$, using a linear scale on the ordinate. These results for high multiplicity Au + Au collisions show a level of adherence to power law behavior that is comparable to what was reported previously for single-particle-inclusive measurements, and demonstrate the persistence of momentum-space coalescence behavior for a larger mean number of participant nucleons.

We do not expect C to be constant across regions where the assumptions underlying the simple momentum-space coalescence model do not hold, for example, where proton and neutron spectra differ. Inclusive neutron [11] and proton [1] spectra have been published for the same system in the case of 0.8A GeV Ne + NaF; no differences within uncertainties are observed at large $p^\perp$, whereas at $p^\perp_{\text{neut}} \sim 0.3$ GeV/c, proton spectra are shifted about 0.1 GeV/c. Coulomb distortion should be more prominent when comparing squared proton densities with deuteron densities than when comparing squared deuteron densities with α densities, and, if anything, the observed deviations at low $p^\perp/A$ show the opposite tendency. Thus, other factors in addition to Coulomb repulsion probably play a role in the low $p^\perp/A$ behavior. For all results that follow (other than the determination of $\mathbf{Q}$, described below), a cut requiring $p^\perp/A \geq 0.2$ GeV/c is imposed. Adherence to the power law deteriorates marginally using the cut $p^\perp/A \geq 0.15$ GeV/c, and with no cut, discrepancies can be large compared with statistical errors.

The center panels of Fig. 1 show the dependence of momentum-space density on $\Phi = |\phi - \phi_R|$, the azimuthal angle of fragment i relative to the event reaction plane as defined by the vector $\mathbf{Q}_i = \sum_{j\neq i}^{M} w(y'_j)\mathbf{p}_j^\perp$ [12], where j runs over all baryonic fragments. The weighting factor $w(y'_j)$ is designed to optimize the correlation of $\mathbf{Q}$ with the reaction plane; for $y' > 0$, we follow the prescription $w(y'_j) = \min(1, y'_j/0.8)$. The reaction plane is determined with an rms resolution of 16° for the events in Fig. 1; this dispersion is negligible in the context of testing the power law as a function of Φ. The normalization factor k is chosen so that the mean ordinate is 1. The solid circles, the solid curves, and the dashed curves have the same meaning as in the upper panels, while the open circles denote the relative density of fragments with $A = 3$ and the dotted curves denote the three-halves power of the deuteron density. Because of the high density of fragments close to the reaction plane in high multiplicity Au + Au collisions, there is a large difference between the density of free protons and the density of all protons be they bound in fragments or not; good agreement with the power law is obtained only if the free

protons are used. Likewise, the density of fragments with mass A' raised to the power A/A' can generally be used interchangeably with the Ath power of the proton density. To illustrate this pattern, we plot $\rho_2^{3/2}$ in place of ρ_1^3 in the center panels of Fig. 1. These findings are consistent with chemical equilibrium being established at the time of freeze-out [5].

There is a considerable body of experimental literature [13–18] describing an increase with A of observables related to the mean in-plane transverse momentum per nucleon $\langle p^x(y)/A\rangle$ [12]. This phenomenon was first suggested by hydrodynamic models [19], in which collective effects were seen more clearly for heavier fragments. The QMD model also exhibits a mass dependence, attributed to early formation and sideward deflection of light and intermediate-mass composites [20]. The mass dependence of $\langle p^x(y)/A\rangle$ persists when the standard $p^\perp$ cut is applied to our data. The lower panels of Fig. 1 show p^x/A densities for protons and deuterons using the same symbols and N units as before. The combination of power law behavior and the asymmetry in the p^x distribution can suffice to explain the A dependence of $\langle p^x(y)/A\rangle$ for $p^\perp/A \geq 0.2$ GeV/c.

The applicability of the momentum-space power law to $\rho(\Phi)$ or $\rho(p^x)$ has not been explored previously. However, using the Boltzmann-Uehling-Uhlenbeck (BUU) model combined with a six-dimensional coalescence prescription for separating masses 1 and 2 from 3 and 4, Koch *et al.* [21] reported reasonable agreement with Plastic Ball $\langle p^x(y)/A\rangle$ data for charges 1 and 2 in 200A MeV Au + Au collisions [14]. BUU is a one-body transport model and is unsuited for treating composite fragment formation unless statistical coalescence is the only important mechanism. Koch *et al.* did not impose a $p^\perp$ cut, but their satisfactory agreement can be reconciled with our findings by noting that Plastic Ball is inefficient for fragments with low $p^\perp/A$ and uncertainties arise from the need to simulate its acceptance; furthermore, the BUU calculation introduced possible model dependence and involved coalescence radii in both position and momentum. Thus our results offer the first quantitative illustration that the A dependence of sideward flow above a $p^\perp$ threshold can be understood, using only experimental data, as a momentum-space coalescence effect. Our data do not exclude the possibility that a more general coalescence prescription determines composite formation at low $p^\perp/A$.

Figure 2 displays the variation of C as a function of multiplicity and rapidity for Au + Au at 1.15A GeV. We define the coalescence coefficient as $C_{AA'} = \rho_A/\rho_{A'}^{A/A'}$, where ρ here denotes track rapidity density. As explained in the discussion of Fig. 1, the power law generally holds equally well for any A' satisfying $A > A' \geq 1$. The observed C is consistent with being independent of rapidity except where spectator fragmentation becomes important, in agreement with the inclusive data from

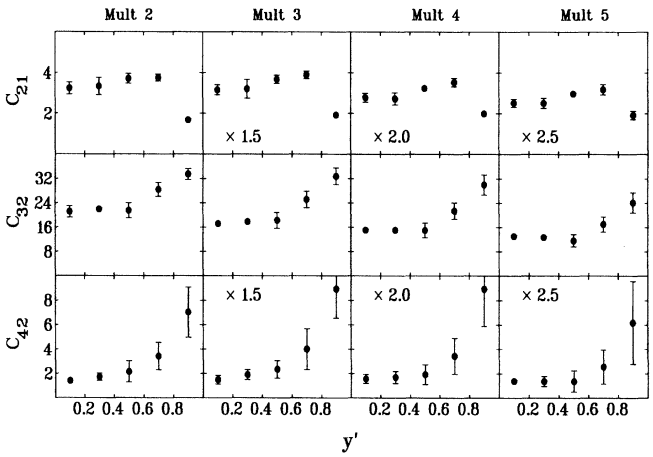

FIG. 2. Coalescence coefficients $C_{AA'}$ as a function of multiplicity and rapidity for light fragments from 1.15A GeV Au + Au collisions. The coefficients are in units of [tracks/(event)(y' unit)]$^{A'/A}$, and were multiplied by 100 times the indicated factors before plotting.

the Bevalac [1]. The decrease in C with increasing multiplicity is a trend that is expected if average spatial effects are considered, as explained previously.

In this Letter, we focus on the extent to which the power law describes the A dependence of $\rho_A(\Phi)$ for light fragments. The $dN/d\Phi$ spectra, as illustrated in the center panels of Fig. 1, have been fitted by functions of the form $1 + \lambda\cos\Phi + \alpha\cos2\Phi$. The second term allows better fits to be obtained for the strongest azimuthal asymmetries, where there are deviations from a cosine shape. The notation λ_A signifies fit values for fragments with mass A, while $\lambda_{AA'}$ signifies fits to the spectrum for mass A' raised to the power of A/A'. In Fig. 3, we present tests of power law behavior through λ comparisons for the full Au + Au sample spanning beam energies between 0.25A and 1.15A GeV. Overall, we conclude that the power law is remarkably consistent in describing fragment flow for $p^\perp/A \geq 0.2$ GeV/c, as parametrized by λ. The most prominent deviation is a tendency for the Ath power of the proton spectra (the open triangles) to overpredict the observed λ values at forward rapidities. The same tendency is not repeated in the deuteron spectra to the power of $A/2$. This deviation has a pattern of dependence on rapidity and multiplicity that is qualitatively consistent with the excess protons having evaporated from the projectile spectator, which is known to experience a sideward deflection in the reaction plane [10].

Important advantages of the EOS TPC are its good particle identification [8], its seamless acceptance, and the fact that it can be simulated with good accuracy. The geometry and target position result in optimum performance at $y' \geq 0$. Using various event generators, we have compared the observables under investigation

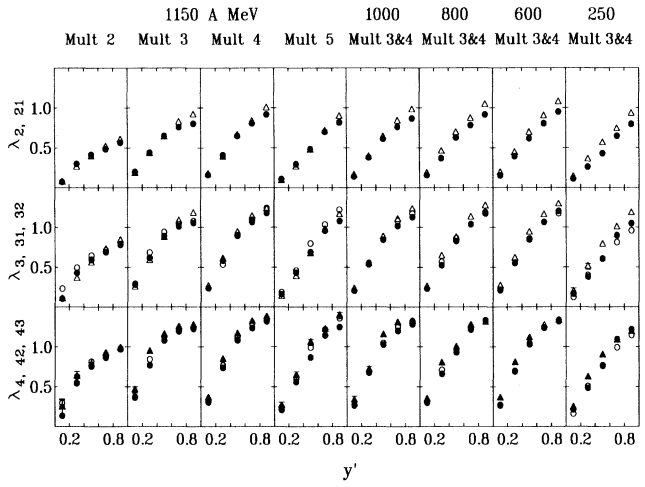

FIG. 3. Sideward flow parameters λ as a function of rapidity. The open triangles indicate λ_{A1}, the parameter based on the Ath power of the proton spectrum. The solid circles indicate both λ_2, the parameter for deuterons, and λ_{A2}, the parameter for the deuteron spectrum to the power of $A/2$. Likewise, the open circles indicate λ_3 and λ_{A3}, and the solid triangles indicate λ_4.

before and after filtering through a detailed GEANT-based simulation of the TPC. We find that detector distortions are comparable to or smaller than the symbol sizes or error bars in Figs. 1 and 3; however, the overall normalization of the $p^{\perp}$ and p^{x} spectra in Fig. 1 is uncertain at the level of 5% to 10%. In Fig. 2, the uncertainties in cases where error bars are larger than the symbol size are predominantly systematic, and are due to uncertainties in particle identification.

The formation of composite fragments is neglected in many event-generating models [3,22,23], including the widely used BUU transport codes which determine only the evolution of one-body phase space. Consequently, the interpretation of comparisons between these models and data can be questioned [3,20]. An important case in point arises in the context of directed flow, which has potential to offer information about the nuclear equation of state [3]. Our findings support the use of models without composite formation to interpret flow measurements, as long as these measurements are in the form of appropriate coalescence-invariant observables [24] with $p^{\perp}/A < 0.2$ GeV/c excluded, and are averaged over all abundant fragment species. Of course, it is important to complement such studies by carrying out more demanding comparisons in which models that treat composite formation [3,4] are tested against a comprehensive set of flow measurements [25]. Overall, we conclude that the simple momentum-space power law consistently describes light participant fragment production at $p^{\perp}/A \geq 0.2$ GeV/c over a remarkably wide range of transverse momentum, azimuth relative to the reaction plane, rapidity, multiplicity, and beam energy in intermediate-energy heavy-ion collisions.

This work is supported in part by the U.S. Department of Energy under Contracts/Grants DE-AC03-76SF00098, DE-FG02-89ER40531, DE-FG02-88ER40408, DE-FG02-88ER40412, and DE-FG05-88ER40437, and by the U.S. National Science Foundation under Grant PHY-9123301.

*Present address: Sung Kwun Kwan University, Suwon 440–746, Republic of Korea.
†Present address: State University of New York, Stony Brook, NY 11794.
‡Present address: Crump Institute for Biological Imaging, Univ. of California, Los Angeles, CA 91776.

[1] H. H. Gutbrod *et al.*, Phys. Rev. Lett. **37**, 667 (1976); M.-C. Lemaire *et al.*, Phys. Lett. **85B**, 38 (1979); B. V. Jacak, D. Fox, and G. D. Westfall, Phys. Rev. C **31**, 704 (1985); S. Hayashi *et al.*, *ibid.* **38**, 1229 (1988); N. Saito *et al.*, *ibid.* **49**, 3211 (1994); J. Barette *et al.*, *ibid.* **50**, 1077 (1994).
[2] S. F. Butler and C. A. Pearson, Phys. Rev. **129**, 836 (1963).
[3] For reviews, see H. Stöcker and W. Greiner, Phys. Rep. **137**, 277 (1986); G. F. Bertsch and S. Das Gupta, *ibid.* **160**, 189 (1988); J. Aichelin, *ibid.* **202**, 233 (1991).
[4] P.-B. Gossiaux *et al.*, Univ. of Nantes Report No. SUBATECH 94-10 (to be published).
[5] A. Z. Mekjian, Nucl. Phys. **A312**, 491 (1978); H. Sato and K. Yazaki, Phys. Lett. **98B**, 153 (1981).
[6] K. G. R. Doss *et al.*, Phys. Rev. C **32**, 116 (1985).
[7] G. Rai *et al.*, IEEE Trans. Nucl. Sci. **37**, 56 (1990).
[8] E. Hjort *et al.*, in *Advances in Nuclear Dynamics,* edited by B. Back, W. Bauer, and J. Harris (World Scientific, Singapore, 1993), p. 63.
[9] M. L. Gilkes *et al.*, Phys. Rev. Lett. **73**, 1590 (1994).
[10] H.-Å. Gustafsson *et al.*, Phys. Rev. Lett. **52**, 1590 (1984).
[11] R. Madey *et al.*, Phys. Rev. Lett. **55**, 1453 (1985).
[12] P. Danielewicz and G. Odyniec, Phys. Lett. **157B**, 146 (1985).
[13] M. B. Tsang *et al.*, Phys. Rev. Lett. **57**, 559 (1986).
[14] K. G. R. Doss *et al.*, Phys. Rev. Lett. **59**, 2720 (1987).
[15] C. A. Ogilvie *et al.*, Phys. Rev. C **40**, 2592 (1989).
[16] J. P. Sullivan *et al.*, Phys. Lett. B **249**, 8 (1990).
[17] G. D. Westfall *et al.*, Phys. Rev. Lett. **71**, 1986 (1993).
[18] A. Kugler *et al.*, Phys. Lett. B **335**, 319 (1994).
[19] H. Stöcker, A. A. Ogloblin, and W. Greiner, Z. Phys. A **303**, 259 (1981); H. G. Baumgardt *et al.*, *ibid.* **273**, 359 (1975).
[20] G. Peilert *et al.*, Phys. Rev. C **39**, 1402 (1989).
[21] V. Koch *et al.*, Phys. Lett. B **241**, 174 (1990).
[22] J. Zhang, S. Das Gupta, and C. Gale, Phys. Rev. C **50**, 1617 (1994).
[23] D. Kahana *et al.*, Kent State University Report No. CNR-007-94 (to be published).
[24] Coalescence causes an increase in flow *per nucleon* with increasing A, as illustrated in Fig. 1. Consequently, a widely used transverse flow observable, $\langle p^{x}/A \rangle$ averaged over all abundant charged species (typically up to ^{4}He), is skewed downward with respect to an unweighted average over all nucleons or over all protons.
[25] M. D. Partlan *et al.*, Report No. LBL-36280 (to be published).